Journal of Engineering Mathematics 21: 349–361 (1987)

Inviscid separated flows of finite extent

N. RILEY
School of Mathematics and Physics, University of East Anglia, Norwich, NR4 7TJ, UK

Received 4 August 1987; accepted 17 August 1987

Abstract. Two-dimensional, inviscid, incompressible flow is considered when the flow region contains a separation bubble of finite length. Within the separation bubble a slender-eddy approximation is employed, whilst outside it small disturbance theory is used to solve the potential-flow equations. The solution is completed by matching the pressure across the vortex sheet that divides the two regions of flow. Solutions are presented for the flow past smooth indentations in an otherwise plane boundary.

1. Introduction

If a steady planar flow, of an inviscid incompressible fluid, contains one or more regions within which the streamlines are closed then in those regions the flow is one with uniform vorticity. This is the celebrated Prandtl–Batchelor result. Proposals to model the wake behind a two-dimensional bluff body using ideas associated with this result have not been entirely successful. By contrast the separated flow past highly swept configurations has been successfully modelled by potential flow in which are embedded vortex sheets. Vorticity which is shed from a leading edge rolls up into a tightly wound spiral and is convected downstream. Since diffusion must always be subordinate to convection such models provide a good representation of the flow in the high Reynolds number limit. By contrast, on the timescale that results in a steady flow, diffusion of vorticity in a flow with closed streamlines will always be effective, no matter how large the Reynolds number. It is this diffusive mechanism which provides the basis for the Prandtl–Batchelor result. Smith [1] has embodied this result in his wake model for the flow past a bluff body. This allows for a wake of infinite extent as the Reynolds number increases indefinitely.

Apart from the classical problem of the wake behind a bluff body there exists the possibility of inviscid modelling for regions of separated flow that are known to be of finite extent. Such flows form the basis of the present paper. Models of this type of flow must build upon the Prandtl-Batchelor result, and examples include flows past cavities or indentations in otherwise planar boundaries. Particular examples of practical importance include the concavities which arise in multi-element aerofoils at the heel of the slat and the cove of the main aerofoil. In a recent review Smith [2] has presented the few examples of flows with finite regions of uniform vorticity which are available in the literature. We are concerned in this paper with separated flow regions which extend much further in the streamwise than the cross-stream direction, and we adopt the slender-eddy approximation of Childress [3] in the separated flow region. For the outer potential flow classical small-disturbance theory is used. A vortex sheet separates the two regions of flow whose shape is represented by a set of Fourier coefficients, these are determined by satisfying the nonlinear equation which arises from continuity of pressure across the sheet. This treatment is different from that of Childress.

The method is an extension of that developed by Riley and Shaw [4] who are concerned with the flow past rectangular cavities, and other situations in which the separation and reattachment points are located at sharp edges. Here we consider smooth indentations, in an otherwise planar boundary, within which we may select the separation and reattachment points. In addition to considering symmetric indentations we consider the flow past a smoothly varying backward-facing step. We present a variety of solutions and we note that, in general, the behaviour close to separation and reattachment is exactly as predicted by the local analysis of Smith [5]. In particular the pressure gradient becomes singular as separation is approached. There are special cases for which this singular behaviour is absent and the role of these as limiting solutions at indefinitely high Reynolds numbers is discussed.

2. The outer flow

We consider the steady, uniform parallel flow of an incompressible, inviscid fluid, speed U_0, past a plane boundary which contains a smooth indentation as shown in Fig. 1. Beyond the indentation the boundary is again planar, and parallel to the boundary upstream of the indentation. The flow is supposed to separate at the point S, and reattach at the point R. There is a separation bubble between S and R, in which the particles move along closed streamlines. This region of separated flow is one within which the flow has uniform vorticity as decreed by the Prandtl–Batchelor theorem; it is separated from the outer flow by a vortex sheet.

As a typical velocity we choose the free-stream speed U_0, with l as a typical length where the points $x = \pm l$ are chosen to lie on the planar sections of the boundary surface. Dimensionless co-ordinates (x, y) are chosen such that the separation (S) and reattachment (R) points are at $x = a, b$ respectively. The vortex sheet, whose location is unknown *a priori*, is represented by

$$y = \varepsilon\eta(x), \quad a \leqslant x \leqslant b, \quad \varepsilon \ll 1. \tag{2.1}$$

In this section we are concerned with the irrotational flow solution outside the region of separated flow. If ψ denotes the stream function then we write

$$\psi = y + \varepsilon\tilde{\psi} + \ldots, \tag{2.2}$$

where the perturbation stream function satisfies, in the small disturbance approximation,

$$\nabla^2\tilde{\psi} = 0, \quad \nabla\tilde{\psi} \to \mathbf{0} \text{ at infinity},$$

$$\left.\frac{\partial\tilde{\psi}}{\partial x}\right|_{y=0} = \begin{cases} -\dfrac{\mathrm{d}\eta}{\mathrm{d}x}, & a \leqslant x \leqslant b, \\ -\dfrac{\mathrm{d}f}{\mathrm{d}x}, & x < a,\ x > b, \end{cases} \tag{2.3}$$

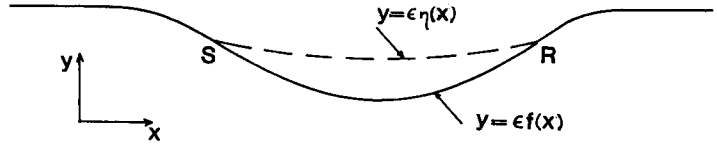

Fig. 1. Definition sketch.

where $y = \varepsilon f(x)$ represents the boundary shape, as shown in Fig. 1, and ∇^2 is the two-dimensional Laplace operator. The solution of the problem posed for $\tilde{\psi}$ in (2.3) may be written as

$$\tilde{\psi}(x, y) = \frac{1}{\pi}\int_{-1}^{1} \frac{\mathrm{d}f}{\mathrm{d}X} \tan^{-1}\frac{y}{x - X}\,\mathrm{d}X + \frac{1}{\pi}\int_{a}^{b} \frac{\mathrm{d}F}{\mathrm{d}X} \tan^{-1}\frac{y}{x - X}\,\mathrm{d}X, \tag{2.4}$$

where

$$-\tfrac{1}{2}\pi \leqslant \tan^{-1}\{y/(x - X)\} \leqslant \tfrac{1}{2}\pi, \quad \text{and} \quad F(x) = \eta(x) - f(x).$$

If we define a pressure coefficient $C_p = (p - p_0)/(\frac{1}{2}\varrho U_0^2)$, where ϱ is the fluid density and p the pressure, then small-disturbance theory gives at the boundary of the outer flow, which is the physical boundary for $x < a$, $x > b$ and the vortex sheet for $a \leqslant x \leqslant b$,

$$\frac{C_p}{\varepsilon} = -2\left.\frac{\partial\tilde{\psi}}{\partial y}\right|_{y=0} = -2\tilde{u}(x, 0), \tag{2.5}$$

with, from (2.4), for $|x| \leqslant 1$

$$\tilde{u}(x, 0) = \frac{1}{\pi}\int_{0}^{\pi} \frac{\mathrm{d}f}{\mathrm{d}X}(\phi)\frac{\sin\phi}{\cos\phi - \cos\lambda}\,\mathrm{d}\phi + \frac{1}{\pi}\int_{0}^{\pi} \frac{\mathrm{d}F}{\mathrm{d}X}(\phi)\frac{\sin\phi}{\cos\phi - \cos\theta}\,\mathrm{d}\phi, \tag{2.6}$$

where in the first of the integrals in (2.4), (2.6) we have written $X = -\cos\phi$, $x = -\cos\lambda$, $0 \leqslant \lambda \leqslant \pi$ and in the second $X = \frac{1}{2}(a - b)\cos\phi + \frac{1}{2}(a + b)$, $x = \frac{1}{2}(a - b)\cos\theta + \frac{1}{2}(a + b)$, $0 \leqslant \theta \leqslant \pi$. Now, using conjugate Fourier series (see, for example, Karamcheti [6]), if we write

$$\frac{\mathrm{d}f}{\mathrm{d}x} = \sum_{n=1}^{\infty} B_n \sin n\lambda, \tag{2.7}$$

where the constants B_n are known, and

$$\frac{\mathrm{d}F}{\mathrm{d}x} = \sum_{n=1}^{\infty} A_n \sin n\theta, \tag{2.8}$$

where the constants A_n are not known, since the shape of the vortex sheet is unknown, then from (2.6), we have

$$\tilde{u}(x, 0) = -\sum_{n=1}^{\infty} B_n \cos n\lambda - \sum_{n=1}^{\infty} A_n \cos n\theta, \quad a \leqslant x \leqslant b,$$

so that for $a \leqslant x \leqslant b$

$$\frac{C_p}{\varepsilon} = 2\sum_{n=1}^{\infty} B_n \cos n\lambda + 2\sum_{n=1}^{\infty} A_n \cos n\theta. \tag{2.9}$$

Outside this range of values of x we make use of the result

$$\int_0^{\pi} \frac{\cos n\phi \, \mathrm{d}\phi}{1 + \mu^2 - 2\mu \cos \phi} = \begin{cases} \dfrac{\pi \mu^n}{1 - \mu^2}, & \mu^2 < 1, \\ \dfrac{\pi}{\mu^n(\mu^2 - 1)}, & \mu^2 > 1, \end{cases}$$

to give, after some manipulation, using equations (2.5) to (2.8),

$$\frac{C_p}{\varepsilon} = \begin{cases} 2\sum_{n=1}^{\infty} B_n\{-\alpha(x)\}^n + 2\sum_{n=1}^{\infty} A_n\{-\beta(x)\}^n, & x < -1 \\ 2\sum_{n=1}^{\infty} B_n \sin n\lambda + 2\sum_{n=1}^{\infty} A_n\{-\beta(\chi)\}^n, & 1 \leqslant x < a, \\ 2\sum_{n=1}^{\infty} B_n \sin n\lambda + 2\sum_{n=1}^{\infty} A_n\{-\beta(\chi)\}^n, & b < x \leqslant 1, \\ 2\sum_{n=1}^{\infty} B_n\{-\alpha(x)\}^n + 2\sum_{n=1}^{\infty} A_n\{-\beta(\chi)\}^n, & x > 1. \end{cases} \tag{2.10a,b,c,d}$$

In equations (2.10a,b), $\alpha(x) = x + (x^2 - 1)^{1/2}$, $\beta(\chi) = \chi + (\chi^2 - 1)^{1/2}$, whilst in (2.10c,d), $\alpha(x) = x - (x^2 - 1)^{1/2}$, $\beta(\chi) = \chi - (\chi^2 - 1)^{1/2}$ and $\chi = 2\{x - \frac{1}{2}(a + b)\}/(b - a)$.

We note that the choice (2.8), through which we represent the vortex-sheet shape $\eta(x)$, is entirely consistent with the local results of Smith [5]. The curvature of the sheet is dominated by

$$\frac{\mathrm{d}^2\eta}{\mathrm{d}x^2} = \frac{\mathrm{d}^2 f}{\mathrm{d}x^2} - \frac{2}{(b - a)\sin\theta} \sum_{n=1}^{\infty} nA_n \cos n\theta, \tag{2.11}$$

which behaves like $(x - a)^{-1/2}$ close to $x = a$, and $(b - x)^{-1/2}$ near $x = b$. This square-root singularity in the curvature is also a feature of Smith's analysis [5] in which the local sheet shape is determined close to a point of separation where the sheet separates an irrotational flow from one with uniform vorticity. The singularity in (2.11) will only be absent for special sets of values of A_n. To obtain an expression for η we integrate (2.8) to get

$$\eta = f + \frac{1}{4}(b - a) \sum_{n=2}^{\infty} A_n \left\{ \frac{\sin(n - 1)\theta}{n - 1} - \frac{\sin(n + 1)\theta}{n + 1} \right\}, \tag{2.12}$$

where the choice $A_1 \equiv 0$ ensures $\eta(a) - f(a) = \eta(b) - f(b) = 0$.

With the solution for the outer flow now completed to $O(\varepsilon)$ for a given $\eta = \eta(x)$ we consider next the rotational flow within the separation bubble.

3. The inner flow

The separated region of flow is one within which the vorticity is uniform, say ω_0. Within this slender region of flow, of scale height $O(\varepsilon)$ the velocity will be $O(\varepsilon^{1/2})$ since the pressure

disturbance must be comparable in order of magnitude with that given by (2.9) in the outer flow region. This in turn indicates that the vorticity will have magnitude $O(\varepsilon^{-1/2})$. Accordingly we introduce new variables Y, Ψ and Ω_0 for this inner region by

$$y = \varepsilon Y, \quad \psi = \varepsilon^{3/2}\Psi, \quad \omega_0 = \varepsilon^{-1/2}\Omega_0. \tag{3.1}$$

Since $\nabla^2\psi = -\omega_0$, the equation satisfied by Ψ is then

$$\varepsilon^2 \frac{\partial^2\Psi}{\partial x^2} + \frac{\partial^2\Psi}{\partial Y^2} = -\Omega_0, \tag{3.2}$$

with

$$\Psi = 0 \text{ on } Y = f(x) \text{ and } Y = \eta(x), \quad a \leqslant x \leqslant b, \tag{3.3}$$

which are the upper and lower bounding streamlines of the region of separated flow.

The leading-order solution of (3.2) and (3.3) is simply

$$\Psi_0(x, Y) = \tfrac{1}{2}\Omega_0 Y^2 + \tfrac{1}{2}\Omega_0\{f(x) + \eta(x)\}Y - \tfrac{1}{2}\Omega_0 f(x)\eta(x), \tag{3.4}$$

which is the slender-eddy solution of Childress [3].

Since $f(x) - \eta(x) \to 0$ as $x \to a, b$ the solution (3.4) is uniformly valid in the region of separated flow, and in particular at its end points. This may be compared with the flows past rectangular cavities considered by Riley and Shaw [4], in which a non-uniformity of the solution (3.4) required correction at the end walls of the cavity.

For this inner flow the pressure coefficient, at the vortex sheet where $\partial\psi/\partial x \ll \partial\psi/\partial y$ is given by

$$\frac{C_p}{\varepsilon} = C - \left(\frac{\partial\Psi_0}{\partial Y}\right)^2, \text{ on } Y = \eta(x), \quad a \leqslant x \leqslant b, \tag{3.5}$$

where C is a constant which is related to the Bernoulli constant, or total head, on the outermost streamline of this inner region.

For a given vortex-sheet shape $\eta = \eta(x)$ the leading-order solution in each of the inner and outer regions has now been completed, see equations (2.4), (3.4). It remains to determine that shape, and this is accomplished by noting that the pressure is continuous across the vortex sheet so that, from (2.9) and (3.5),

$$2\sum_{n=1}^{\infty} B_n \cos n\lambda + 2\sum_{n=2}^{\infty} A_n \cos n\theta + \tfrac{1}{4}\Omega_0^2 \mathscr{F}^2(\theta) - C = 0, \tag{3.6}$$

with, from (2.12),

$$\mathscr{F}(\theta) = \frac{1}{4}(b - a)\sum_{n=2}^{\infty} A_n \left\{\frac{\sin(n-1)\theta}{n-1} + \frac{\sin(n+1)\theta}{n+1}\right\}. \tag{3.7}$$

For given values of B_n ($n = 1, 2, \ldots$), a, b, the constants A_n($n = 2, 3, \ldots$), and hence the sheet shape, may be determined from equation (3.6). Our method of solution is discussed in the next section.

4. Solution procedure

The equation which is to be satisfied, namely (3.6), we write in the form

$$\Phi(\{A_j\}, \{B_j\}, a, b, \Omega_0, C, x) = 2\sum_{n=1}^{\infty} B_n \cos n\lambda + 2\sum_{n=2}^{\infty} A_n \cos n\theta + \tfrac{1}{4}\Omega_0^2 \mathscr{F}^2(\theta) - C = 0. \tag{4.1}$$

The solutions we have obtained, and present below, relate either to an indentation which is symmetric about $x = 0$ or asymmetric in the form of a smoothly varying backward-facing step. Before describing the method of solution of (4.1) in detail we outline our general strategy. For a given bounding surface the first step is to calculate the Fourier coefficients B_j in (2.7). In all the cases considered we have calculated the first 80 of these coefficients. Now, equation (4.1) is nonlinear and there is strong evidence from our numerical experiments, and those of other investigators, that the solution is unique when the bounding surface is non-symmetric. However, for symmetric cases we have found that symmetric solutions are not unique. For these symmetric bounding surfaces we have been unable to find any asymmetric solutions by the present methods. We can advance no reason why such solutions should be precluded, but we are unaware of any asymmetric solutions for symmetric configurations that have been obtained by others. So, for asymmetric cases, we have obtained the unique solution by treating C, Ω_0 and the Fourier coefficients A_j ($j \geqslant 2$) as unknown quantities in (4.1); but for symmetric cases we have obtained a range of solutions by varying Ω_0 or C and solving (4.1) for $A_j (j \geqslant 2)$ and C, or Ω_0.

In order to solve (4.1) we have terminated the Fourier series (2.8) at $n = N - 1$ say, and satisfied the equation at either N or $N - 1$ collocation points depending upon whether we are dealing with an asymmetric or symmetric boundary. We have chosen the collocation points to be at equal intervals of θ in $0 \leqslant \theta \leqslant \pi$. This has the advantage of a higher density of collocation points close to the points of separation and reattachment than over the central parts of the region in question. The equations we must solve are, then,

$$\Phi_i(A_2, \ldots, A_{N-1}, \{B_j\}, a, b, \Omega_0, C, x_i) = 0, \tag{4.2}$$

for $i = 1$ to $N - 1$ or N. The method of solution of the set of equations (4.2) that we have adopted is a straightforward multivariate extension of the Newton-Raphson procedure for the iterative solution of a single equation in one unknown. We implement this as follows for the asymmetric cases. Suppose that the vector $\mathbf{X} = (A_2, \ldots, A_{N-1}, C, \Omega_0)$ is the solution vector, with $\mathbf{X}^r$ an approximation to it, in some sense. We then have

$$\mathbf{O} = \mathbf{F}(\mathbf{X}) \doteq \mathbf{F}(\mathbf{X}^r) + J \cdot (\mathbf{X} - \mathbf{X}^r), \tag{4.3}$$

where J is the Jacobian matrix with $\partial F_i/\partial X_j$ in its ith row and jth column. If the right-hand side of (4.3) is set equal to zero we may reasonably expect that a better approximation will be obtained, from the solution of the resulting equation, as

$$\mathbf{X}^{r+1} = \mathbf{X}^r - J^{-1} \cdot \mathbf{F}(\mathbf{X}^r). \tag{4.4}$$

Our iterative procedure is based upon (4.4). For the symmetric flows we have considered the method has proved to be robust and, starting with the solution for which $\Omega_0 = 0$ rapid convergence is achieved. For the asymmetric solutions we present, difficulty was experienced in obtaining an adequate initial approximation $\mathbf{X}^0$. This was resolved by starting with a case which is close to the backward-facing step of Riley and Shaw [4]. No difficulty was experienced in continuing to other solutions.

5. Calculated results

We consider first solutions associated with the boundary

$$f(x) = \begin{cases} 0.005 - \operatorname{sech} 6x + \delta\{e^{-130(x+0.75)^2} + e^{-130(x-0.75)^2}\}, & |x| \leqslant 1, \\ 0, & |x| > 1. \end{cases} \tag{5.1}$$

where δ is a constant.

For $\delta = 0$ we seek solutions which are symmetric with $a = -b$. With the separation and reattachment points fixed a solution for $\Omega_0 = 0$ is readily found since equations (4.2) are then linear. For this free-streamline solution the pressure is constant along the vortex sheet. We can then increase the range of solutions by steadily increasing the value of the vorticity Ω_0. We do not present detailed solutions for this case, but we do note some features which are common to the solutions for $\delta \neq 0$ in (5.1). First, the solutions of (4.2) are found to be multivalued. This is illustrated in Fig. 2 for the case $b = 0.8$. As a consequence, beyond a certain value of Ω_0 we must change our strategy, and treat that quantity as an unknown as we steadily increase C. Also in Fig. 2 we show the maximum value of η namely $\eta(0)$. We see that this quantity increases almost linearly with C, whilst Ω_0 gradually declines, once its maximum value has been attained. All the solutions obtained exhibit singular behaviour at the points of separation and reattachment. This behaviour reflects that of the sheet curvature inferred from (2.11). The local solutions of Smith [5] show that as $x \to a-$, $\varepsilon^{-1}\mathrm{d}C_p/\mathrm{d}x = \mathrm{O}\{(x-a)^{-1/2}\}$ whilst as $x \to a+$, $\varepsilon^{-1}\mathrm{d}C_p/\mathrm{d}x = \mathrm{O}\{(x-a)^2\}$, with analogous behaviour at $x = b$. Our numerical solutions clearly reflect these features, and we shall encounter them again when $\delta \neq 0$. The singular behaviour outlined above is exactly as in the Kirchhoff free-streamline solutions. The framework of the Sychev–Smith theory of laminar separation therefore carries over unchanged. This means that the singular behaviour of the inviscid solution must be suppressed if it is to represent the infinite Reynolds number limit of a real flow. This implies, from (2.11), that solutions for which $\Sigma_{n=2}^{\infty} nA_n = 0$ may be of special importance. For this present case, with $\delta = 0$ the only such solution is when $b = -a = 1$. The vortex sheet is then a planar extension of the boundary $y = 0$, $|x| > 1$; along it the pressure is constant and $\Omega_0 \equiv 0$. Herwig [7] encountered a similar situation in his study of

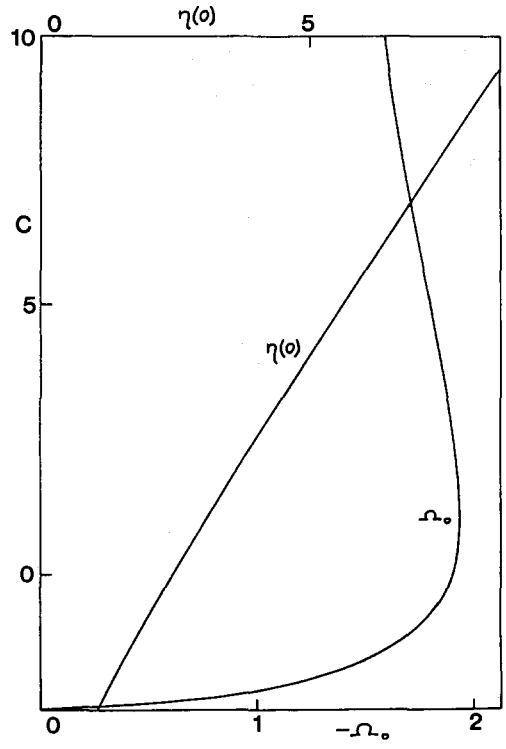

Fig. 2. The variation of C and $\eta(0)$ with Ω_0 for the case $\delta = 0$ (equation 5.1).

the flow past a rectangular cavity, and in order to analyse a more interesting case he introduced a hump on the upstream and downstream lips of the cavity. It is in that spirit we now consider flows with $\delta \neq 0$ in (5.1).

We have chosen to work with $\delta = 0.5$ and in Fig. 3 we show the pressure distribution for attached symmetric flow in our small-disturbance treatment. This case provides a wider variety of flows than that considered above. We again concentrate on symmetric flows, and we find that smooth separation is possible, that is there are solutions for which $\Sigma_{n=2}^{\infty} nA_n = 0$ for the ranges $-1 < x \lesssim -0.78$, $-0.64 \lesssim x \lesssim -0.51$. For the points at the ends of these ranges we have $\Omega_0 = 0$ which correspond therefore to smoothly separating free-streamline

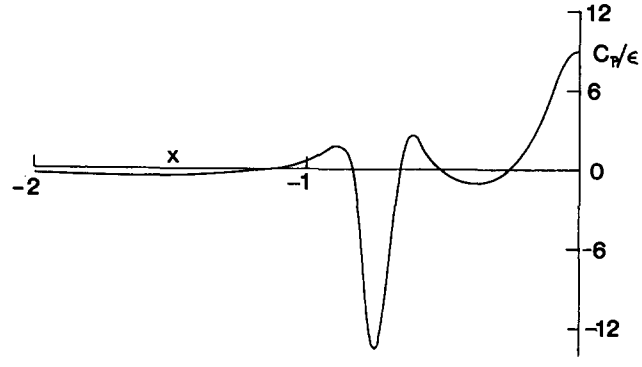

Fig. 3. The attached-flow pressure distribution for the case $\delta = 0.5$.

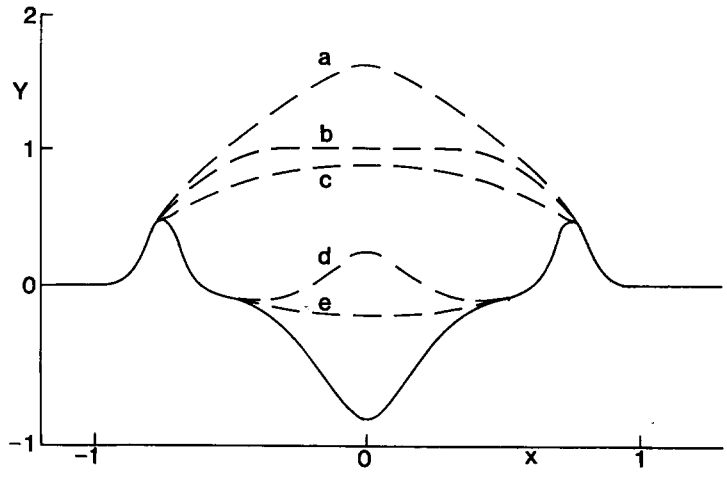

Fig. 4. Vortex-sheet shapes for $\delta = 0.5$: (a) $a = -0.785$, $\Omega_0 = -1.53$, smooth separation; (b) $a = -0.7835$, $\Omega_0 = 0$, smooth separation; (c) $a = -0.75$, $\Omega_0 = 0$, singular separation; (d) $a = -0.53$, $\Omega_0 = -3.91$, smooth separation; (e) $a = -0.507$, $\Omega_0 = 0$, smooth separation.

flows. Not all of these solutions are physically realistic since for some, close to $x = -1$, we find that the vortex sheet intersects the boundary. For flow past a finite bluff body, for example a circular cylinder, it is known that the Kirchhoff free-streamline flow with smooth separation is the correct representation of the potential flow. It is not clear that this is still true when the separated region is of finite extent. But, to be sure, the high-Reynolds-number triple-deck theory is known to be consistent with such a solution. We present five sets of results for $\delta = 0.5$. Four of these correspond to smooth separation. The vortex-sheet shapes associated with these are shown in Fig. 4 with the corresponding pressure distributions in Fig. 5. In Fig. 4 the sheet shapes (a) and (b) correspond to smooth separation with $a = 0.785, -0.7835, \Omega_0 = -1.53, 0$ respectively. The corresponding pressure distributions in Fig. 5 (a, b) are closely similar up to the point of separation. Thereafter they do of course differ considerably, with substantial pressure variations along the vortex sheet in the former case. A neighbouring free-streamline solution, with $a = -0.75$ is shown as (c) in Fig. 4. The corresponding pressure distribution in Fig. 5 (c) shows very clearly the development of the singularity in the pressure distribution as separation is approached. The remaining two solutions are for smooth separation with $a = -0.53, -0.507$ and $\Omega_0 = -3.91, 0$ respectively. Again the pressure distributions are similar up to the point of separation, but there are substantial differences in the variation along the vortex sheets, which reflect the considerable differences to be seen in the sheet shapes.

We turn next to asymmetric flows associated with the smooth, backward-facing step given by

$$f(x) = \begin{cases} 1, & x < -1, \\ \frac{1}{2}[1 - \tanh\{15(x + 0.75)\}], & |x| \leqslant 1, \\ 0, & x > 1. \end{cases} \tag{5.2}$$

For this case a starting solution is not easy to find. The solutions obtained by Riley and Shaw [4] for the case of a sharp backward-facing step, that is a discontinuous transition, were

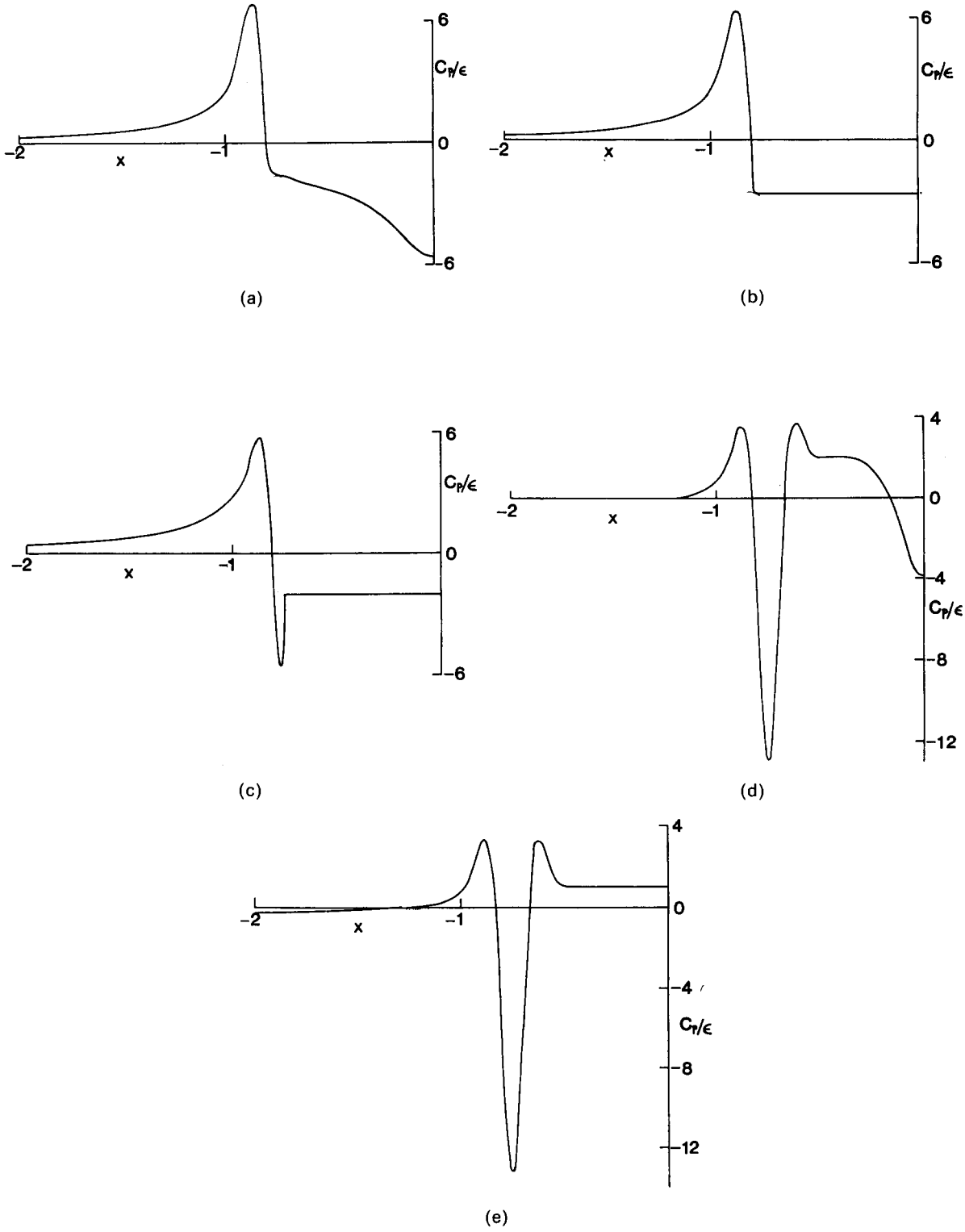

Fig. 5. Pressure distributions for the case $\delta = 0.5$ which correspond to the vortex-sheet shapes shown in Fig. 4.

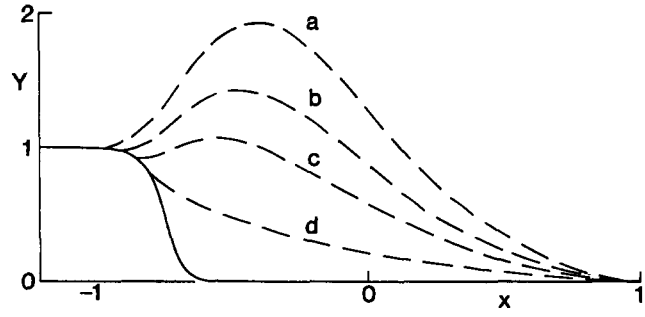

Fig. 6. Vortex-sheet shapes for the backward-facing step, equation (5.2): (a) $a = -1.0, \Omega_0 = -2.99$; (b) $a = -0.9$, $\Omega_0 = -3.33$; (c) $a = -0.85, \Omega_0 = -3.59$; (d) $a = -0.805, \Omega_0 = 0$.

relatively easy to find and it is such a solution that we have adopted as a starting solution here. We have fixed the reattachment point as $b = 1.0$ and in Fig. 6 we show vortex-sheet shapes for four different positions of separation. The corresponding pressure distributions are shown in Fig. 7. As we have noted above, for such asymmetric flows there is strong numerical evidence to suggest that the solutions are unique when the separation and reattachment positions are fixed. When separation is close to the top of the step the solutions are qualitatively similar to the solution presented by Riley and Shaw [4] for the flow past a sharp step. The behaviour of the pressure distribution close to separation does, however, differ. In Figs. 7 (a to d) the pressure distributions all show the characteristics of Smith's local solution [5], with singular behaviour in the pressure gradient as separation is approached and a smoothly varying pressure gradient beyond separation. This same, expected, behaviour is also observed at the reattachment point. The sequence of solutions we present for (5.2) terminates with the free-streamline solution (d). As we have noted none of the solutions shown in Fig. 6 exhibit smooth separation. Indeed, it may well be that the only solution which separates smoothly leaves $x = -1$ as a continuation of the plane boundary $Y = 1$ without reattachment.

We note that all the results we have presented have been carried out for both $N = 41$ and $N = 81$. Very little difference is observed between the two sets, and those reported here are for the larger value of N.

One feature which has emerged from our calculations, and was also observed by Riley and Shaw [4], is that for symmetric geometrical configurations the solutions are not unique. This is also true of the relatively few solutions that are available for such flows when the slender approximation is not appropriate. For example Sadovskii [8], Sadovskii and Sinitsyna [9], Herwig [7] and Pullin [10] present a range of solutions for particular symmetric configurations, whilst Saffman and Tanveer [11] find only one solution for a particular asymmetric configuration.

6. Conclusions

In this paper we have outlined a method for calculating inviscid, incompressible flows in which there are separation bubbles of finite extent on a smooth, indented surface. All the flows we have considered are slender and the success of the method, which is not difficult to implement and is economical in computer time, is based upon the simple approximate

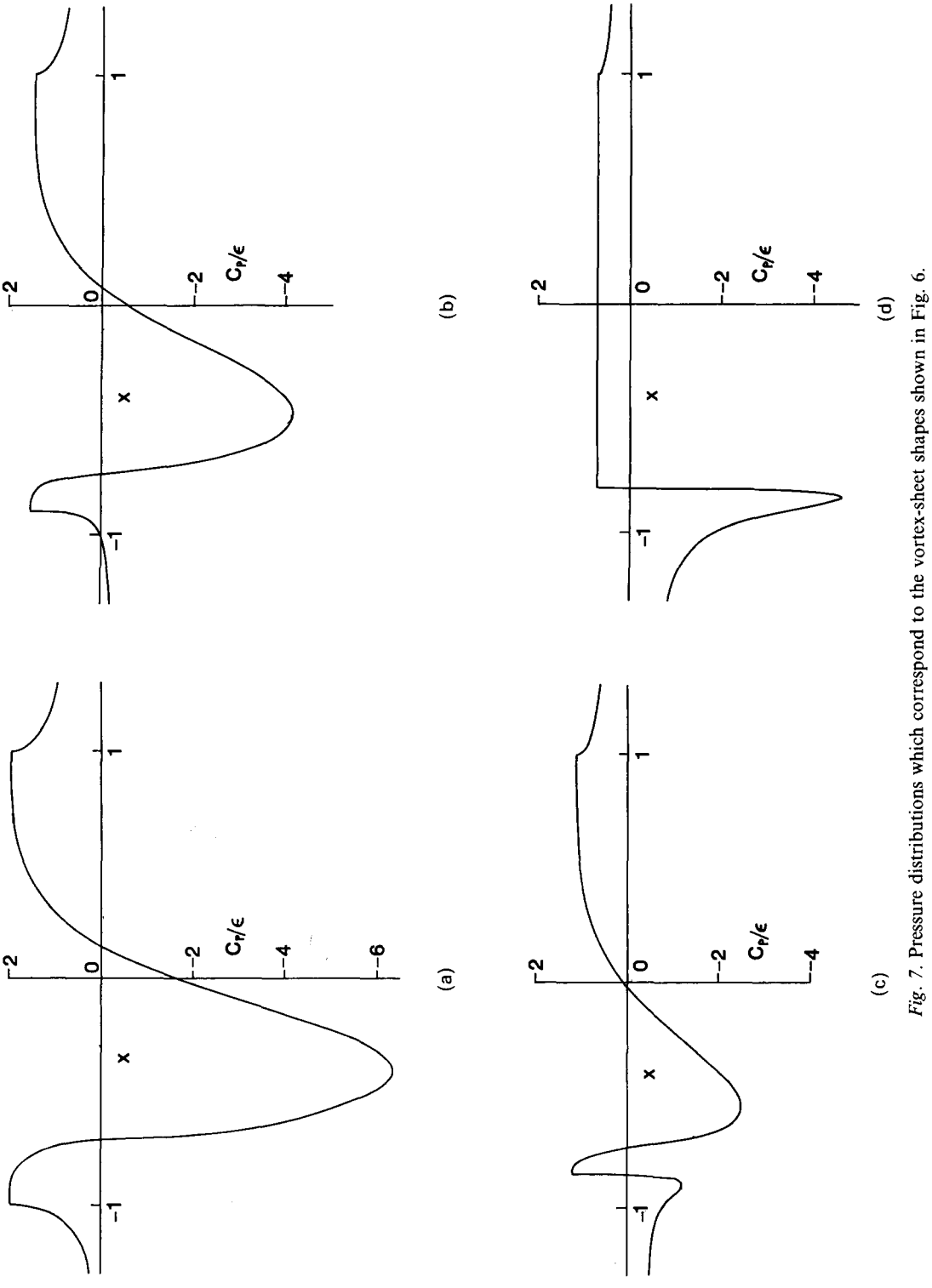

Fig. 7. Pressure distributions which correspond to the vortex-sheet shapes shown in Fig. 6.

solution of Childress [3] for slender eddies within which there is a rotational flow with uniform vorticity. For symmetric configurations we have demonstrated that the solutions are not unique, and that it is possible to find solutions which do not exhibit singular behaviour at separation. Some of these are smoothly-separating free-streamline flows. Although we expect the inviscid solution, which is to be the high-Reynolds-number limiting solution, to exhibit non-singular behaviour at separation it is still necessary to exercise a choice between those available. For these finite regions of separated flow we cannot expect the smoothly-separating free-streamline solution to be the appropriate high-Reynolds-number limit solution. To determine the appropriate solution, in particular the level of vorticity Ω_0 in the separated flow region, it is necessary to demonstrate the consistency of the viscous boundary layer which surrounds the region with that value of Ω_0. A method by which this may be achieved in principle has been described by Riley [12].

References

1. F.T. Smith, A structure for laminar flow past a bluff body at high Reynolds number, *J. Fluid Mech.* 155 (1985) 175–191.
2. J.H.B. Smith, Vortex flows in aerodynamics, *Ann. Rev. Fluid Mech.* 18 (1986) 221–242.
3. S. Childress, Solutions of Euler's equations containing finite eddies, *Physics Fluids* 9 (1966) 860–872.
4. N. Riley and R.E. Shaw, An inviscid model of planar separated flows of finite extent, *RAE TR86070* (1986).
5. J.H.B. Smith, The representation of planar separated flow by regions of uniform vorticity. In: H.G. Hornung and E.-A. Müller (eds), *Vortex Motion*, pp. 157–172, Braunschweig/Wiesbaden: Vieweg (1982).
6. K. Karamcheti, *Principles of Ideal-fluid Aerodynamics*, Wiley (1966).
7. H. Herwig, Die Anwendung der asymptotischen Theorie auf laminare Strömungen mit endlicher Ablösegebieten, *Z. Flugwiss: Weltraumforsch*, 6 (1982) 266–279.
8. V.S. Sadovskii, Vortex regions in a potential stream with a jump of Bernoulli's constant at the boundary, *J. Appl. Math. Mech.* 35 (1971) 729–735.
9. V.S. Sadovskii and N.P. Sinitsyna, Mixed flow of an ideal fluid on a plane containing a recess, *Fluid Dyn.* 18 (1985) 306–309.
10. D.I. Pullin, A constant-vorticity Riabouchinsky free-streamline flow, *Quart. J. Mech. Appl. Math.* 37 (1984) 619–631.
11. P.G. Saffman and S. Tanveer, Prandtl–Batchelor flow past a flat plate with a forward-facing flap, *J. Fluid Mech.* 143 (1984) 351–364.
12. N. Riley, High Reynolds number flows with closed streamlines, *J. Engg. Math.* 15 (1981) 15–27.